A High Temperature, Frequency Output Silicon Temperature Sensor

Shane Rose, Mark Hahn
Quartzdyne Inc.
4334 W. Links Drive
Salt Lake City, Utah 84120
Phone: (801) 266-6958 Fax: (801) 266-7985

Abstract

Precision high temperature sensors often require temperature compensation. Quartzdyne pressure transducers use a temperature sensitive quartz crystal for compensation. In an effort to shrink transducer packaging, and increase reliability; a prototype frequency output temperature sensor was designed using a 0.8um silicon bulk CMOS process.

The 250°C operational sensor is based on a PTAT current generator. The design uses high temperature design techniques that were proven reliable in prior Quartzdyne ASIC's. The output frequency is 34kHz at 30°C, with a sensitivity of 100Hz/°C and achievable accuracy of ±0.3°C from 25°C to 200°C. This paper will review the sensor's characteristics, including the output linearity, hysteresis, accelerated aging and temperature cycling to demonstrate the performance and long term reliability and repeatability of the sensor.

Keywords: Temperature Sensor, CMOS, High Temperature Electronics

Introduction:

Quartzdyne pressure transducers are based on quartz crystal sensors and a quartz reference clock for frequency counting. The pressure sensor's sensitivity to temperature requires compensation, which is currently accomplished with a temperature sensitive crystal that is not exposed to the pressure medium. Transducers are calibrated at a set of pressures and temperatures. A polynomial curve fit is used to estimate pressure and temperature.

Commercial voltage or current output silicon temperature sensors have been available for many years. Most do not function at high temperature and require extra components to complete the analog to digital conversion. A custom frequency output silicon temperature sensor reduces circuit component count, by eliminating the analog to digital converter and a few passives components. The output frequency can be counted using the current reference clock source and a Quartzdyne frequency counter ASIC.

The sensor can be implemented two ways; a discrete ASIC that allows the sensor to be located closer to the pressure crystal, and an integrated form that allows the sensor to be included in the oscillator ASIC. Both implementations create the option to replace the current temperature crystal on future Quartzdyne pressure transducers.

A prototype silicon temperature sensor based on a proportional to absolute temperature (PTAT) current source has been designed and tested. A frequency output is obtained by using a relaxation oscillator to convert the PTAT current to frequency. The device was fabricated in a 0.8µm bulk CMOS process using established and proven high temperature design techniques [1,2,3,4].

The sensitivity is about 100Hz/°C at low temperatures, above 200°C it decreases significantly. The sensor is capable of achieving ±0.3°C accuracy, between 30°C and 200°C with a 2nd order curve fit. A calibration accuracy of ±3.5°C for operation at 225°C is possible with a 3rd order curve fit. Two parallel aging studies demonstrated the drift to be approximately ±3°C; one at 250°C for 36 days and another at 225°C for 48 days.

The hysteresis was measured to be 0.2°C on three of four sensors. After 10 cycles from ambient to 200°C, most sensors shifted less than 0.5°C.

Circuit Description:

The circuit uses two identical diodes biased at different currents (Figure 1), generating a difference voltage that is PTAT. An amplifier and a resistor are configured in a feedback loop to generate a PTAT current source. Equation 1 defines the current; M and N represent the number of vertical substrate PNP transistors that are within Q1 and Q2.

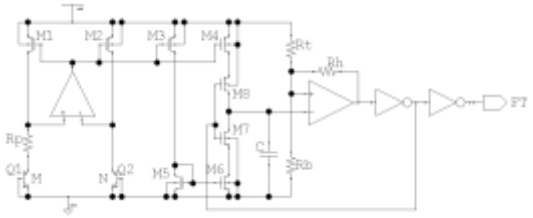

Figure 1 Temperature Sensor Schematic

$$Eq.1 \qquad I_{ptat} = \frac{kT}{R_p} \mathrm{Ln}\left(\frac{M}{N}\right)$$

Equation 1 defines the PTAT current that is used to charge and discharge a capacitor in a

relaxation oscillator. The circuit operates in two phases, charging and discharging. During the charging phase the comparator output is high, R_h is in parallel with R_t, M8 is on and M7 is off. Once the capacitor voltage is charged to V_{Trise} (Equation 4) the comparator output switches signaling the discharge phase. During the discharge phase the comparator output is low, R_h is in parallel with R_b, M8 is off, M7 is on. Once the capacitor voltage is discharged to V_{Tfall} (Equation 5) the phase shifts back to the charging phase.

The circuit oscillates between the two phases creating a frequency represented by Equation 2. Differentiating Equation 2 with respect to temperature gives the sensitivity shown in Equation 3. The rising and falling edge triggers are set by R_b, R_t and R_h according to Equations 4-6.

$$Eq.2 \quad F[Hz] = \frac{kTLn\left(\frac{M}{N}\right)}{2RCV_{pp}}$$

$$Eq.3 \quad S\left[\frac{Hz}{°C}\right] = \frac{kLn\left(\frac{M}{N}\right)}{2RCV_{pp}}$$

$$Eq.4 \; V_{Trise} = V_{dd}\frac{R_b}{\frac{R_tR_h}{R_t+R_h}+R_t}$$

$$Eq.5 \; V_{Tfall} = V_{dd}\frac{\frac{R_bR_h}{R_b+R_h}}{\frac{R_bR_h}{R_b+R_h}+R_t}$$

$$Eq.6 \; V_{pp} \approx V_{Trise} - V_{Tfall}$$

The test module is shown in Figure 2. The left half is the temperature sensor and the right half is the voltage regulator and signal driver. These modules were built on a standard Quartzdyne hybrid substrate for convenience and known packaging reliability.

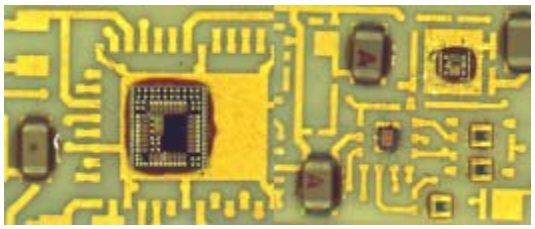

Figure 2 Temperature Sensor Hybrid Circuit

Calibration:

Modules were calibrated in an air current isolated hot chuck that is capable of holding the temperature to ±0.1°C. (Figure 3) The temperature was swept from ambient to 250°C taking a point every 25°C. The output frequencies were measured with an HP5313A frequency counter using its internal reference clock source and the 100 KHz filter on.

Figure 3 Calibration Hot Chuck

A sample set of typical responses to temperature is shown in Figure 4. Room temperature sensitivity is roughly 110Hz/°C; it slowly decreases to approximately 95Hz/°C at 185°C. The non-linearity above 200°C significantly limits the sensors achievable accuracy as shown in Figures 5-7.

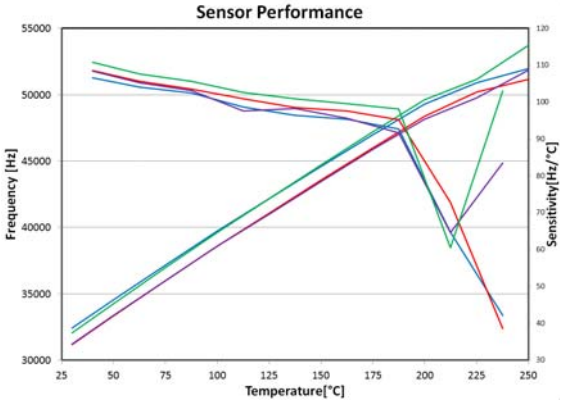

Figure 4 Sensor Performance

$$Eq.7 \quad T[°C] = \sum_{0}^{n} {C_n}^n F^n$$

Polynomial calibration coeficients of the form shown in Equation 7 are obtained by using a least-means-squared curve fitting algorithm. The calibration error is determined by subtracting the calculated from the true measured temperatures.

A 2nd order curve fit achieves ±0.3°C accuracy at 200°C and lower. First order curve fits

do not produce comparable results. Because a 3rd order curve fit had reasonable results at 225°C max temperature, this type of curve fit is used to make a performance comparison.

Coefficients focusing on different temperature ranges (30°C to Tmax) were used to show the performance capabilities vs maximum temperature. Maximum temperatures of 200°C and lower have accuracies better than ±0.3°C. Above 200°C the accuracy is an order of magnitude worse, approximetely ±3.5°C. Below 150°C three of four sensors are capable of 0.1°C accuracy (Figures 5-7).

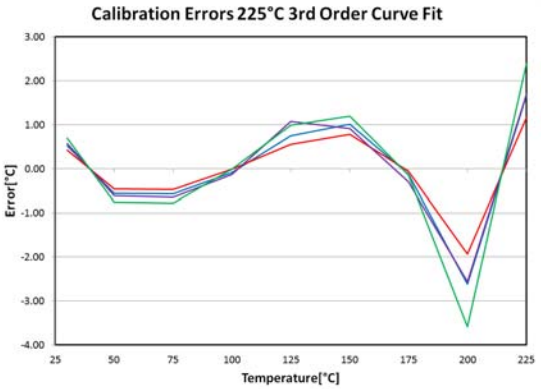

Figure 5 225°C Calibration Error

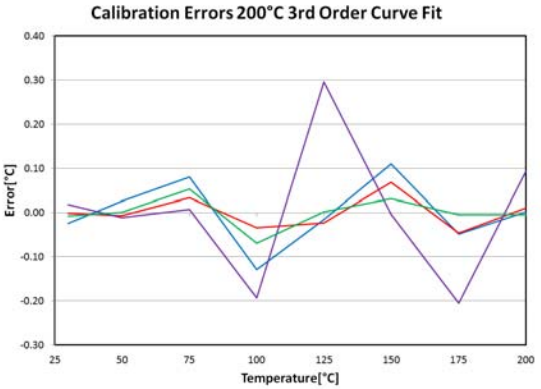

Figure 6 200°C Calibration Error

Aging Characteristics

Six sensors were aged at 225°C for 48 days; four more sensors were aged at 250°C for 36 days. The samples were buried in steel shot inside a glass-baking pan to reduce the oven-induced temperature variations. This method has been shown to reduce the device under test (DUT) temperature deviation to only a few tenths of a degree C. A thermocouple mounted on a centrally located DUT is used compensate the remaining temperature changes. Hourly measurements are averaged over one day to obtain one data point.

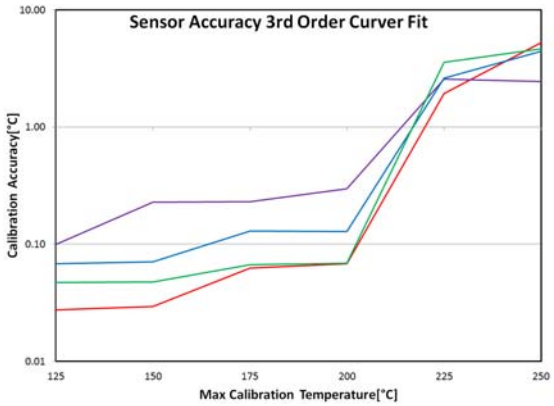

Figure 7 Performance Comparison

The data are plotted in Figures 8 and 9. The 225°C drift slows down after about ten days on most sensors. One sensor ages in the positive direction and levels off after approximately 30 days. The magnitude of the drift is approximately ±3°C.

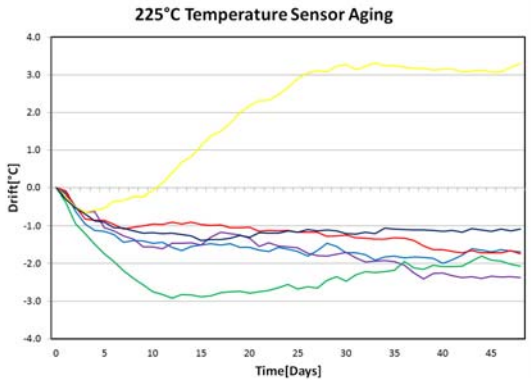

Figure 8 225°C Aging

At 250°C, all the samples drifted negative and continued to drift the entire 36 days. Unfortunately, the oven malfunctioned and the test was terminated. The worst-case sample drifted about -3°C, while the best case was -1.0°C.

Hysteresis & Temperature Cycling

A set of four sensors received a hysteresis loop from ambient to 250°C in 75°C steps. Next, the sensors endured ten temperature cycles from ambient to approximately 200°C, and data were recorded at each ambient point. The results of these two experiments are shown in Figures 9 and 10.

The difference between ramp up and ramp down calculated temperatures is hysteresis and is plotted in Figure 10. Most sensors show roughly 0.2°C or less hysteresis. However one sensor is significantly worse at 0.9°C.

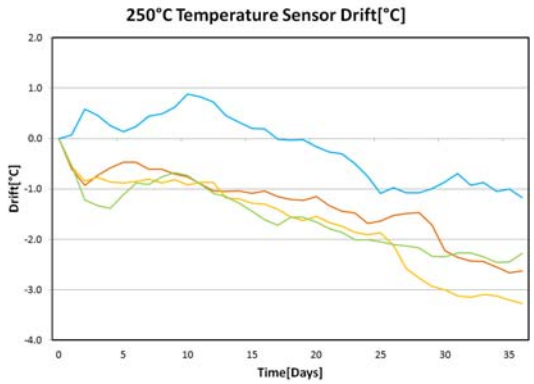

Figure 9 250°C Aging

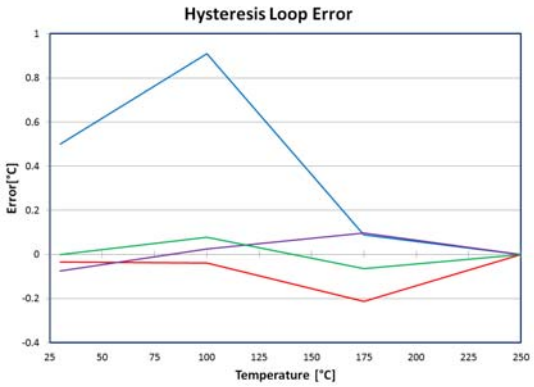

Figure 10 Hysteresis Loop Error

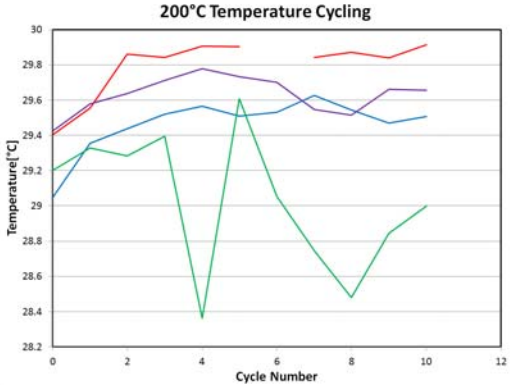

Figure 11 200°C Temperature Cycling

Temperature cycling shows that three of four sensors shifted between 0.25°C and 0.5°C after the 10 cycles. These three sensors were fairly well behaved. One of the four sensors did not behave as well. It showed shifts between -0.8°C and +0.4°C with multiple changes in direction. All sensors showed some changes in direction with increasing cycles, but the one sensor was more dramatic. See Figure 11 for details.

Conclusion:

A 250°C operational prototype silicon frequency output temperature sensor that is capable of ±0.3°C accuracy up to 200°C is shown. Long-term 250°C/225°C aging demonstrated ±3°C errors over one month period. While the 250°C aging data suggests that the sensor will continue to degrade, the 225°C data shows a slowing of aging after 10-30 days.

Most sensors show a 0.2°C error on a 250°C hysteresis loop. One sensor showed a much larger 0.9°C error. During the ten temperature cycles, most sensors behave somewhat consistently showing less than 0.5°C errors.

There are two methods of implementation, integrated and discrete. When integrated, the sensor would be included within the Quartzdyne Oscillator ASIC. As a discrete component, the small size allows it to be placed closer to the pressure sensor reducing transient errors. Both options allow for smaller pressure transducers.

Acknowledgments

The authors would like to thank Muris Beslagic & Ryan Roush for wire bonding modules, Trang Dang for soldering cables to the modules and Stephen Reynolds for recording data.

References

[1] Richard Brown & Koucheng, Wu. “Scaling CMOS Design Rules for High-Temperature Latchup Immunity”

[2] Shoucair, F.S. “Design Considerations in High Temperature Analog CMOS Integrated Circuits.” IEEE Transactions on Components, Hybrids, and Manufacturing Technology, Sept 1986, pp 242-251.

[3]Pect,Micheal. “The influence of Temperature on Integrated Circuit Failure Mechanisms.”, Quality and Reliability Engineering International, May-June 1992, vol. 8, No 3. Pp 167-175

[4] Rose, Shane. “A 225°C Rated ASIC for Quartz based Downhole Transducers” HITEN 2007, (www.quartzdyne.com)

[5] Rose Shane, Watts Mark, “Quartzdyne ASIC Developments”, HITEN 2009 (www.quartzdyne.com)

[6] Rose Shane, “High Temperature CMOS Reliability and Drift” HITEC 2010, (www.quartzdyne.com)

[7] Buddhika Abesingha, Gabriel A. Rincon-Mora et all, “Voltage Shift in Plastic-Packaged BandGap References” IEEE Transactions on Circuits and Systems, Vol 49, No 10 October 2002.

[8] K. M. Schlesier, S. A. Keneman, and R. T. Moonet, “Piezoresistivity effects in plastic-encapsulated integrated circuits,” RCA Rev., vol. 43, pp 590-607, Dec 1982